AFML-TR-74-133

FRACTURE MECHANICS TESTS AND ANALYSES OF THE AEDC APTU STORAGE VESSEL MATERIAL

TECHNICAL REPORT AFML—TR—74—133

OCTOBER 1974

AIR FORCE MATERIALS LABORATORY
AIR FORCE SYSTEMS COMMAND
WRIGHT—PATTERSON AIR FORCE BASE, OHIO 45433

REPORT DOCUMENTATION PAGE		READ INSTRUCTIONS BEFORE COMPLETING FORM
1. REPORT NUMBER AFML-TR-74-133	2. GOVT ACCESSION NO.	3. RECIPIENT'S CATALOG NUMBER
4. TITLE *(and Subtitle)* FRACTURE MECHANICS TESTS AND ANALYSES OF THE AEDC APTU STORAGE VESSEL MATERIAL		5. TYPE OF REPORT & PERIOD COVERED June 1973 - June 1974
		6. PERFORMING ORG. REPORT NUMBER
7. AUTHOR(s) Allan W. Gunderson		8. CONTRACT OR GRANT NUMBER(s)
9. PERFORMING ORGANIZATION NAME AND ADDRESS Air Force Materials Laboratory (AFML/MXE) Air Force Systems Command Wright-Patterson Air Force Base, Ohio 45433		10. PROGRAM ELEMENT, PROJECT, TASK AREA & WORK UNIT NUMBERS Project No. 7381 Task No. 738106
11. CONTROLLING OFFICE NAME AND ADDRESS		12. REPORT DATE October 1974
		13. NUMBER OF PAGES 48
14. MONITORING AGENCY NAME & ADDRESS*(if different from Controlling Office)*		15. SECURITY CLASS. *(of this report)* Unclassified
		15a. DECLASSIFICATION/DOWNGRADING SCHEDULE
16. DISTRIBUTION STATEMENT *(of this Report)* Approved for public release; distribution unlimited.		
17. DISTRIBUTION STATEMENT *(of the abstract entered in Block 20, if different from Report)*		
18. SUPPLEMENTARY NOTES		
19. KEY WORDS *(Continue on reverse side if necessary and identify by block number)* Fracture Proof Test Crack Growth Rate		

20. ABSTRACT *(Continue on reverse side if necessary and identify by block number)*

A test program to evaluate cyclic crack growth rates and residual strengths of flawed panels has been completed. The test specimens were from representative high pressure air storage tanks similar to those used in the AEDC APTU test facility. The test results reported herein, coupled with the proof test performed at AEDC, provide the data base to use a proof test logic methodology for estimating the minimum cyclic life of the storage tank field.

FOREWORD

The test effort described herein was conducted on large test specimens cut from salvaged high pressure storage vessels. The physical size of the specimens required a test machine of a large capacity located at the Wheel and Brake Test Facility, Air Force Flight Dynamics Laboratory. The cooperation and assistance of Mr. Don Huffman, AFFDL/FED was greatly appreciated. The testing support on this effort was very competently provided by Mr. Richard Marton and Mr. Kenneth Smith of the University of Dayton Research Institute.

This report was prepared by Mr. Allan W. Gunderson of the Air Force Materials Laboratory for research accomplished under Project 7381, Task 738106.

Research was performed during the period of June 1973 through June 1974.

TABLE OF CONTENTS

TABLES

ILLUSTRATIONS

SECTION I
INTRODUCTION AND BACKGROUND

The new ultra-high velocity Aerodynamic and Propulsion Test Unit (APTU) facility at the Arnold Engineering Development Center required a large volume of high pressure air for operation. The magnitude of the high pressure storage tank field required is shown in Figure 1. The test facility is of the "blowdown" type and therefore, the air storage tanks experience a cyclic pressure variation. The tanks were reclaimed from surplus Atlas missile launch facilities. No records of cyclic history were available except for the original proof test data obtained from the manufacturer.

The use of pressure vessels in circumstances other than they were originally designed for, coupled with the fact that they were not designed to meet ASME pressure vessel codes, posed some serious questions about their safety and applicability. The pressure vessels to be incorporated into the high pressure storage field were cleaned, non-destructively inspected, and given a hydrostatic proof test by AEDC personnel to the levels shown in Table I.

A combination of linear elastic fracture mechanics analysis coupled with the proof test qualification testing was selected to provide a cyclic life estimate for the pressure vessels. The proof test has been used for many years as a usage qualification test and a quality control device. However, it was not until the fracture mechanics principles were developed and applied in the 1960's that cyclic life expectancy could be calculated by a crack growth analysis. A comprehensive report on this analysis methodology was given by Tiffany and Masters in 1964 (Reference 1). A design monograph developed under NASA sponsorship was completed by Tiffany in 1970 (Reference 2).

The linear elastic fracture mechanics solutions used in the service life analysis are based on the stress intensity (K) approaches initially developed by Irwin (References 3 and 4). Two basic solutions were

1

used (1) for the through-crack in a plate:

$$K = \sigma \sqrt{\pi a} \tag{1}$$

where:

K = stress intensity
  psi $\sqrt{in}$
  σ = stress, psi
  a = half crack length, inches

(2) for the part-through-crack in a plate also developed by Irwin (Reference 5) in 1962:

$$K = 1.1\sigma \sqrt{\pi \frac{a}{Q}} \tag{2}$$

where:

Q = Flaw Shape/Stress Level Parameter (Figure 2)
  a = crack depth into thickness (critical dimension)

These equations were used to determine the flaw sizes possible to be in the pressure vessel at the proof test stress level. A crack growth analysis was then used to estimate the number of cycles required for the flaw to grow to a critical size at the maximum operating pressure on to a through-crack which would cause tank leakage. The crack growth analysis was based on:

$$da/dN = F(\Delta K) \tag{3}$$

where:

da/dN = crack growth for cycle
  ΔK = stress intensity range

which was proposed initially by Paris in 1964 (Reference 6).

SECTION II

TEST MATERIAL, SPECIMENS, AND METHODS

The air storage field has a total of 96 tanks which are made by
several suppliers out of different materials. A listing of the basic
materials, manufacturers, and construction data is given in Table II.
The highest strength material used was the USS T-1 steel at a nominal
yield strength of 100 ksi. The major portion of the test effort shown
in Table III was on this alloy because the majority of the vessels were
constructed from it and because the higher strength could possibly have
a lower fracture toughness. Also, the other alloys have been previously
used in pressure vessels built to ASME codes. Figure 3 shows a simplified
sketch of a Foster-Wheeler constructed vessel.

The surface flaw specimens were of the design shown in Figure 4.
The flaw was machined in by electrical discharge machining. The flaw
shape is shown in Figure 5. It is semicircular in shape and it was
attempted to provide as sharp a tip as possible. Ideally, a notch
should be extended by fatigue crack growth but a fatigue machine of
sufficient capacity (500,000 lbs) was not available. The EDM leaves a
brittle surface which may compensate somewhat for the lack of a fatigue
crack extension. The test machine used was a one million pound tension,
three million pound compression Baldwin-Southwark located in the AFFDL
Wheel and Brake Test Facility (Figure 6).

Three areas of interest were evaluated in the surface flaw tests:
the base metal to provide a comparison point, the weld metal to check on
adequacy and quality, and the heat affected zone (HAZ) at the weld/ base
metal interface to see if any degradation occurs due to the high thermal
input to this area. The gage section was lightly etched with a nital
solution to show the exact weld area (Figure 7). Care was taken to keep
the nital solution out of the crack tip.

In addition to the room temperature tests, low temperature tests on
the surface flaw specimens were conducted using an insulating chamber

of foam surrounding the gage section into which liquid nitrogen was sprayed. The temperature readout was by three copper/constantan thermocouples driving a pushbutton Brown/Electrix recorder. One thermo-couple was located on the back face, one on the front face, and the third inserted into the tip of the eloxed notch. The temperature was stabilized for a minimum of five minutes before testing.

Crack opening displacement (COD) of the surface flaw specimen was plotted versus the applied load on Moseley X-Y recorder. A typical example is shown in Figure 8. The COD gage used was the standard four strain gage bridge model described in ASTM Test Method E-399 (Reference 7).

Fatigue crack growth rate (da/dn) tests were conducted on the T-1 steel using the compact specimen (Figure 9). An MTS Servo hydraulic test machine was used at a frequency of 15 Hertz and an "R" ratio $\frac{\text{LOAD MIN}}{\text{LOAD MAX}}$ of 0.1. The environment was laboratory air at a nominal 45 to 55% relative humidity.

The compact specimen was used in a two-inch thickness in an attempt to obtain a fracture toughness value on the A. O. Smith A225 type steel used in the head hemispheres.

The stress corrosion cracking susceptibility of T-1 steel was checked by use of compact specimens precracked and then dead weight loaded in a stress corrosion test frame (Figure 10). The corrosive environment in these sustained load tests was distilled water, a possible internal tank environment due to condensation on the tank walls.

SECTION III
RESULTS AND DISCUSSION

The fracture tests using the surface flaw specimen showed no
appreciable toughness degradation from room temperature to -50°F. A
listing of these test results is given in Table IV. A change in fracture
appearance is shown in Figure 11. The fracture at room temperature was
predominately shear mode whereas the colder temperatures produced a
planar, flat fracture indicative of a plain strain condition. In all
cases, the load at fracture produced stresses in the net area (gross
area minus flaw area) above the yield strength of the material and
usually approached the net area ultimate tensile strength of the
material. This is a very important point to emphasize as it shows the
amount of "forgiveness" in the material. This means that localized
stress concentrations which can occur in any welded assembly, can
theoretically yield during the proof pressure cycle which acts as a
stress relief cycle. The T-1 steel from the Foster-Wheeler tanks had a
calculated K critical of over 130 ksi$\sqrt{in}$ and no observed degradation in
toughness down to the -50°F test temperature. This compares favorably
with data in the Aerospace Structural Metals Handbook originally reported
by Barson (Reference 8) which shows a K_{IC} value for T-1 steel (A-517-F)
at -50°F of 120 ksi$\sqrt{in}$. Data by Gentilicore, Pense, and Stout (Reference
9) give similar results for T-1 steel (A-517-F) in weldments, heat
affected zones, and base metal. This work points out two interesting
points, one, the base metal has the lowest toughness in the tests
conducted and secondly, a stress relief after welding reduced the
fracture toughness of the weld and heat affected zone to that of the
base metal. The Atlas construction drawings for the T-1 steel vessels
called out a stress relief after welding which probably caused the
uniformity in test results between the weldment, HAZ, and base metal in
these tests.

The surface flaw fracture tests on the A302B steel showed no
degradation in toughness from room temperature to -50°F. The lower
tensile strength reduced the calculated "K" maximum as expected even
though the ratio of net stress to ultimate strength increased.

5

Fatigue crack growth rates for the T-1 steel conducted on a limited number of tests indicate a rate on the low side of a range described by Barsom, et.al (Reference 10). The results were obtained in a laboratory air environment which would probably model the environment on the internal surfaces of a pressure vessel. By plotting the crack growth rate data as a function of stress intensity range, Figure 12 is readily usable for the crack growth analysis in the next section of this report.

Stress corrosion cracking is not usually a problem with steels in these lower strength ranges, nevertheless, two compact tension specimens of T-1 steel were tested in a distilled water environment. They were loaded at stress intensities of 80 and 90 ksi$\sqrt{in}$ and the tests were discontinued after over 3500 hours with no failures. The specimens were then pulled apart and the fracture surfaces were examined. In Figure 13, the slight growth exhibited by the specimen loaded to 90 ksi$\sqrt{in}$ can be noted.

Compact fracture toughness specimens on the A. O. Smith pressure head steel were tested but the results were invalid as the load versus crack opening displacement curves exhibited excessive curvature which indicates gross plastic flow. This behavior is desirable in a pressure vessel, however, as it allows yielding to occur and excessively high stress concentrations due to misalignment to be relieved during a proof test. The contraction of the specimen sides from this plastic flow can be seen in Figure 14.

SECTION IV
SERVICE LIFE ANALYSIS

The actual service cyclic life following a proof test is dependent on many factors. Among these factors are proof pressure, operating pressure, crack growth rates, fracture toughness, stress corrosion susceptibility, and environment. The following analysis will be made on the T-1 steel on which the majority of the test effort was expended.

The first item calculated in this analysis was the critical crack length in the material at the maximum operating pressure. This indicated whether a crack could become critical before it grew through the thickness.

On Figure 15, a plot of tank pressure versus critical crack length for the Foster-Wheeler Tank is presented based on the basic fracture mechanics equation.

$$K = \sigma \sqrt{\pi a};$$

where:

K = stress intensity factor

σ = nominal hoop stress

a = half crack length

The stress to pressure conversion was based on thin wall pressure vessel equation:

$$\sigma = \frac{Pr}{T}$$

where:

P = internal pressure

r = mean cylinder radius

T = wall thickness

The stresses thus calculated will be slightly reduced from those calculated by using the more applicable thick wall formulas, although the effect on the analysis would be small.

7

It can be noted from Figure 15 that the critical crack lengths for a maximum operating pressure of 4000 psi is about five thicknesses for the T-1 steel. This would indicate the crack should grow through the thickness of the wall and leak before reaching a critical size. The segment marked safe crack growth range is the growth from the proof test maximum flaw size to the size where possible stress corrosion cracking could occur. This crack growth would be from a part-through-crack or an imbedded flaw. The stress corrosion tests on the T-1 steel indicated the sustained load cracking threshold stress intensity is above 90 ksi$\sqrt{\text{in}}$.

The number of pressure cycles from the proof stress flaw size, assumed to be a part-through-crack, to a through the thickness crack can be projected by using the crack growth rate data previously generated. In Tables V and VI, two crack geometries of a/2c (flaw depth/flaw surface length) of 0.1 and 0.25 are calculated for the nominal hoop stresses at 4000 psi maximum. The data thus obtained can be plotted as the K/Kproof ratio (alternately, pressure or stress ratio) versus cycles. It is apparent from the data plotted in Figure 16 that the flaw shape has very little effect on the number of pressure cycles required to penetrate the thickness from the proof test flaw size. The a/2c of 0.25 flaw penetrated through the thickness below the minimum stress corrosion cracking level of 90 ksi$\sqrt{\text{in}}$, whereas, the a/2c of 0.1 flaw just reached the 90 ksi$\sqrt{\text{in}}$ stress intensity as it grew through the thickness. This indicates stress corrosion would not be a problem because air leakage and thus discovery of the flaw would occur below the stress corrosion cracking level.

The result of using a higher pressure cycle can be seen in Figure 17. In this graph flaws of a/2c = 0.1 are projected to a through-crack using a 4000 to 1200 psi pressure cycle and a 5000 to 1200 psi pressure cycle. The higher pressure cycle reaches a stress intensity greater than the minimum K_{ISCC} value determined, which means sustained load crack growth could be possible. It can be noted that regardless of the method of crack growth, the crack will grow through the thickness before reaching the critical stress intensity.

From the shape of the flaws grown cyclically through the thickness in Reference 1, it is assumed the flaw shape of 0.25 would be more applicable to this problem. Longer flaws or discontinuities would also show up more readily during the x-ray and magnetic particle inspections carried out on these tanks as indicated on Table I, and therefore would most likely be repaired before being put in service.

The cyclic growth curves are not projected beyond the point of a through-crack which will produce air leakage. It is presumed a regular schedule of inspections will be followed to ascertain if any of the tanks have developed through-cracks. Also, only cracks occurring in the cylindrical portion of the storage tanks have been analyzed. This is the region of the highest calculated stresses barring discontinuities which could cause stress concentrations in other areas.

Application of the proof test/crack growth logic relates the proof test stress to the operating stress through the appropriate fracture mechanics equation. Thus, it can be seen from Equation 1, the flaw size screened by the proof test in the area of a stress concentration is smaller than the normal stress field flaw by:

$$\frac{1}{K_t^2} \cdot \text{a normal stress field}$$

A crack growth service life analysis at a stress concentration would vary only slightly from the normal stress field life analysis, although the possibility exists that at a stress concentration the flaw could reach critical before growing through the thickness.

Another feature of the proof test crack growth logic that will be of value is the "resetting" ability. At some future date when a significant portion of the projected life has been expended, a reproof test to the original AEDC level will again screen for flaws down to the proof test flaw size and thus "reset" the crack growth analysis.

SECTION V
CONCLUSIONS

1. The part-through-crack fracture tests conducted on the T-1 and the A302-B steels indicate no fracture toughness degradation down to -50°F. The fractures in each instance occurred only after the yield strength of the material was exceeded. The toughness variation of the T-1 steel between the base metal, weld metal, and heat affected zone was not significant.

2. The stress corrosion cracking threshold for T-1 steel is above 90 ksi$\sqrt{in.}$ No problems with sustained load cracking appears likely.

3. The pressure cycles to a through-crack in the Foster Wheeler 250 cu. ft. tanks based on the proof test/crack growth rate analysis are on the order of 40,000 cycles for a 4000 to 1200 psi range. By application of the proof test/crack growth methodology the cyclic life in the other pressure vessels can be determined.

4. A factor of safety should be applied to the predicted cyclic lives calculated. This will then represent the cyclic usage available before a reproof test would be desirable.

REFERENCES

1. C. F. Tiffany and J. N. Masters, Applied Fracture Mechanics from ASTM STP 381 Fracture Toughness Testing and its Application 1964.

2. C. F. Tiffany, "Fracture Control of Metallic Pressure Vessels," NASA SP-8040 1970.

3. G. R. Irwin, "Analysis of Stresses and Strains Near the End of a Crack Traversing a Plate," Journal of Applied Mechanics, 1957.

4. G. R. Irwin, "Fracture" Handbuch der Physik, Vol VI, Springer, Berlin, 1958.

5. G. R. Irwin, "The Crack Extension Force for a Part Through Crack in a Plate" Journal of Applied Mechanics, 1962.

6. P. C. Paris, "The Fracture Mechanics Approach to Fatigue," Fatigue: An Interdisciplinary Approach Proceedings 10th Sagamore Conference, Syracuse University Press, 1964.

7. ASTM Book of Standards E-399-72.

8. J. M. Barsom, "Relationship Between Plane Strain Ductility and K_{IC} for Various Steels," ASME Journal of Engineering for Industry, Vol 93, November 1971.

9. V. J. Gentilicore, A. W. Pense, and R. D. Stout, "Fracture Toughness of Pressure Vessel Steel Weldments," Welding Journal Supplement, August 1970.

10. J. M. Barsom, E. J. Imhof, and S. T. Rolfe, "Fatigue Crack Propagation in High Yield Strength Steels," Engineering Fracture Mechanics, Vol. 2, 1971.

TABLE I

SUMMARY OF APTU HIGH PRESSURE GAS STORAGE VESSELS

Manufacturer	Press. Mfg.	Rating AEDC	Vol. Ft3	Qty.	Manufacturer's Inspection Hydro psi	X-ray yes	X-ray no	MPI # yes	MPI # no	AEDC Inspection Hydro psi	X-ray yes	X-ray no	MPI # yes	MPI # no
Foster Wheeler	6600	5170	180	19	11,220		x	x		8,800		x	x	
		5160	250	41	11,220		x	x		8,800		x	x	
		3500	625	2 *	7,480					—				
Struthers Wells	6600	4800	180	5	11,220	x			x	8,100		x	x	
		4800	250	5	11,220	x			x	8,100		x	x	
Taylor Forge	6600	4010	180	10	11,220	x		x		8,100		x	x	
	6000	5000	850	2 *	9,600	x		x				x		x
A. O. Smith	6600	5000	180	5	11,220	x		x		8,800		x	x	
		5000	250	8	11,220	x		x		8,800		x	x	

* Not Used In The Present APTU Facility   # Magnetic Particle Inspection

TABLE II

CONSTRUCTION MATERIALS
ATLAS PRESSURE VESSELS

Manufacturer	Cylinder	Hemi-Heads	Nozzles	Welds
Foster-Wheeler	USS T-1*	USS T-1	A106-GRF	L61(A-1010 X 10)
Struthers Wells	USS T-1	USS T-1	USS T-1	L60(A1811 X 15) L61(A1010 X 10)
Taylor Forge	A 302-GR B	A302-GR B	A302-GR B	Not Specified
A. O. Smith	A.O.S. Spec 1146a Laminated	A.O.S. Spec 1146a	A.O.S. Spec 1146a	SW-120A

* USS T-1 Conforming to ASTM A517- Grade F

13

TABLE III

APTU PRESSURE VESSEL MATERIAL TEST PROGRAM

Type Specimen	Manufacturer	Material	Flaw Location	Test Temperature		
				Room	0°	-50°
Surface Flaw	Foster-Wheeler	T-1	Base Metal	X	X	
			Weld	X	X(X)	XX
			Heat Affected Zone (HAZ)	X	X	
	Struthers Wells	T-1	Weld	XX	XX	X
	Taylor Forge	A302B	Weld	XX	XX	X
Crack Growth Rate	Foster-Wheeler	T-1	Weld Metal	XXX		
Compact Fracture	A. O. Smith	≈ A225	Base Metal	XXX		
Stress Corrosion	Foster-Wheeler	T-1	Weld Metal	XX		

X - Indicates one specimen.

TABLE IV

SURFACE FLAW SPECIMEN FRACTURE TEST RESULTS

A302B - UTS 95 ksi   Y.S. 82.5 ksi
T-1 - UTS 117.5 ksi   Y.S. 106.5 ksi

Material	Specimen	Location	Test Temp.	Failure Load (KIPS)	a Crack Depth	Crack Length 2C	Width	Thickness	Gross Stress	Net Stress	K Critical
A302B	1	Weld	Room	808	0.61	2.1	6.85	1.36	86.6	96.5	112.4
"	2	"	"	804	0.6	2.11	6.86	1.37	85.4	94.5	111
"	3	"	0°	813	0.61	2.16	6.87	1.37	86.2	95.7	112
"	4	"	0°	802	0.62	2.23	6.88	1.37	85.0	94.8	113
"	5	"	-50°	814	0.63	2.16	6.85	1.37	86.5	96.5	114
T-1	*S1	"	Room	598	0.4	1.86	7.0	0.84	101.8	111.0	117
"	S2	"	"	604	0.41	1.86	7.0	0.84	102.5	112.2	119
"	S3	"	0°	616	0.42	1.88	7.0	0.85	103.5	113.7	121
"	S4	"	0°	623	0.41	1.88	7.0	0.84	106.0	116.8	123
"	S5	"	-50°	626	0.42	1.90	7.0	0.84	106.4	117.4	125
"	1	Base Metal	RT	955	0.67	2.13	6.97	1.37	99.8	111.3	132
"	2	"	RT	963	0.63	2.17	6.87	1.37	102	114.2	134.5
"	3	Weld HAZ	0°	915	0.64	2.17	6.87	1.34	99.5	111	132
"	4	Weld	0°	978	0.65	2.19	6.89	1.39	102	114	135
"	5	Base Metal	0°	922	0.63	2.16	6.89	1.31	102	114	134
"	6	Weld HAZ	RT	967	0.63	2.20	6.93	1.28	109	122.5	143.5
"	7	Weld	0-4~ -50-1~ RT-Failure	1003	0.64	2.18	6.9	1.34	108.6	120	143.5
"	8	Weld	-55	983	0.65	2.18	6.88	1.29	111	125	146.5
"	9	"	-55	885	0.64	2.17	6.87	1.31	98.4	110	129.3

* T-1 Steel Specimens with "S" designate the Struthers Wells Vessel.
  The remainder of the specimens are from the Taylor Forge Vessels.

TABLE V

CRACK GROWTH ANALYSIS

(4000-1200 PSI Pressure Cycle a/2c=0.1)

FOSTER-WHEELER VESSEL

T-1 Steel Wall Thickness 2.437 Inches

Hoop Stress at 8800 psi Proof Pressure - 65.5 ksi

$K_{critical}$ - 130 ksi$\sqrt{in}$ Q = 1.0

a/2c = 0.1

$$K = 1.1\sigma \sqrt{a/Q} \sqrt{\pi}$$

$$a = \frac{130}{65.5} \frac{\sqrt{1}}{\sqrt{\pi}} \, 1.1$$

a = 1.04 Inches at Proof Pressure

a	K	ΔK	σ	Δa	Growth Rate	Δ Cycles	Total Cycles	K_i/K_{Proof}
1.04	59.5		30					
1.20	64	44.8	30	.16	2.1×10^{-5}	7619	43991	.492
1.40	69	48.3	30	.2	2.5	8000	36372	.531
1.60	74	51.8	30	.2	2.9	6897	28372	.569
1.80	78.4	54.9	30	.2	3.3	6060	21475	.603
2.0	82.6	57.9	30	.2	3.7	5405	15415	.635
2.2	86.6	60.7	30	.2	4.2	4762	10010	.666
2.4	90.5	63.4	30	.2	4.5	4444	5248	.696
2.437	91.2	63.9	30	.037	4.6	804	804	.702

TOTAL PRESSURE CYCLES TO THROUGH CRACK - 43991

TABLE VI

CRACK GROWTH ANALYSIS

(4000-1200 PSI Pressure Cycle a/2C = 0.25)

FOSTER-WHEELER VESSEL

T-1 Steel Wall Thickness 2.437 Inches

Hoop Stress at 8800 psi Proof Pressure - 65.5 ksi

$K_{critical}$ - 130 ksi$\sqrt{in}$ Q = 1.38

a/2c = 0.25

$$K = 1.1\sigma\ \sqrt{a/Q}\ \sqrt{\pi}$$

$$a = \frac{130}{65.5}\sqrt{\frac{1.38}{\sqrt{\pi}\ 1.1}}$$

a = 1.44 Inches at Proof Pressure

a	Q_{CONST}	a/Q	$K_{4000\ psi}$	$\sigma_{4000\ psi}$	ΔK	Δ Cycles	Total Cycles	$\dfrac{K_{initial}}{K_{Proof}}$
1.44	1.38	1.04	59000	29800				.466
1.50		1.09	60500		42.4	3880	46880	.481
1.60		1.16	62500		43.8	5900	43000	.495
1.70		1.23	64400		45.0	5550	37100	.509
1.80		1.3	66100		46.3	5260	31550	.525
1.90		1.38	68200		47.8	4760	26290	.539
2.0		1.45	70000		49.0	4540	21530	.55
2.1		1.52	71500		50.0	4260	16990	.564
2.2		1.59	73100		51.2	4080	12730	.577
2.3		1.67	75000		52.5	3780	8650	.59
2.4		1.74	76600		53.6	3570	4870	.594
2.437		1.77	77100		54	1300	1300	

TOTAL PRESSURE CYCLES TO THROUGH CRACK - 46880

17

TABLE VII

CRACK GROWTH ANALYSIS
(5000-1200 PSI Pressure Cycle a/2C = 0.1)

FOSTER-WHEELER VESSEL

T-1 Steel Wall Thickness 2.437 Inches

Hoop Stress at 8800 psi Proof Pressure - 65.5 ksi

$K_{critical}$ - 130 ksi$\sqrt{in}$ Q = 1.0

a/2c = 0.1

$$K = 1.1\sigma \; \sqrt{a/Q} \; \sqrt{\pi}$$

$$a = \frac{130}{65.5} \sqrt{\frac{1}{\pi}} \; 1.1$$

a = 1.04 Inches at Proof Pressure

a	K_{max}	ΔK	σ	Δa	Growth Rate	ΔCycles	Total Cycles	K_i/K_{Proof}
1.04	74	56.7	37250				22471	.57
1.20	79.5	60.4		.16	4.1×10^{-5}	3900	18571	.61
1.40	86	65.4		.2	4.9×10^{-5}	4080	14491	.66
1.60	92	70		.2	5.7×10^{-5}	3510	10981	.71
1.80	97.5	74.1		.2	6.4×10^{-5}	3120	7861	.75
2.00	103	78.3		.2	7.4×10^{-5}	2700	5161	.79
2.2	108	82		.2	3.0×10^{-5}	2500	2661	.83
2.4	112.5	85.5		.2	8.9×10^{-5}	2250	411	.87
2.437	113.5	86.3		.037	9.0×10^{-5}	411		.87

TOTAL PRESSURE CYCLES TO THROUGH CRACK - 22471
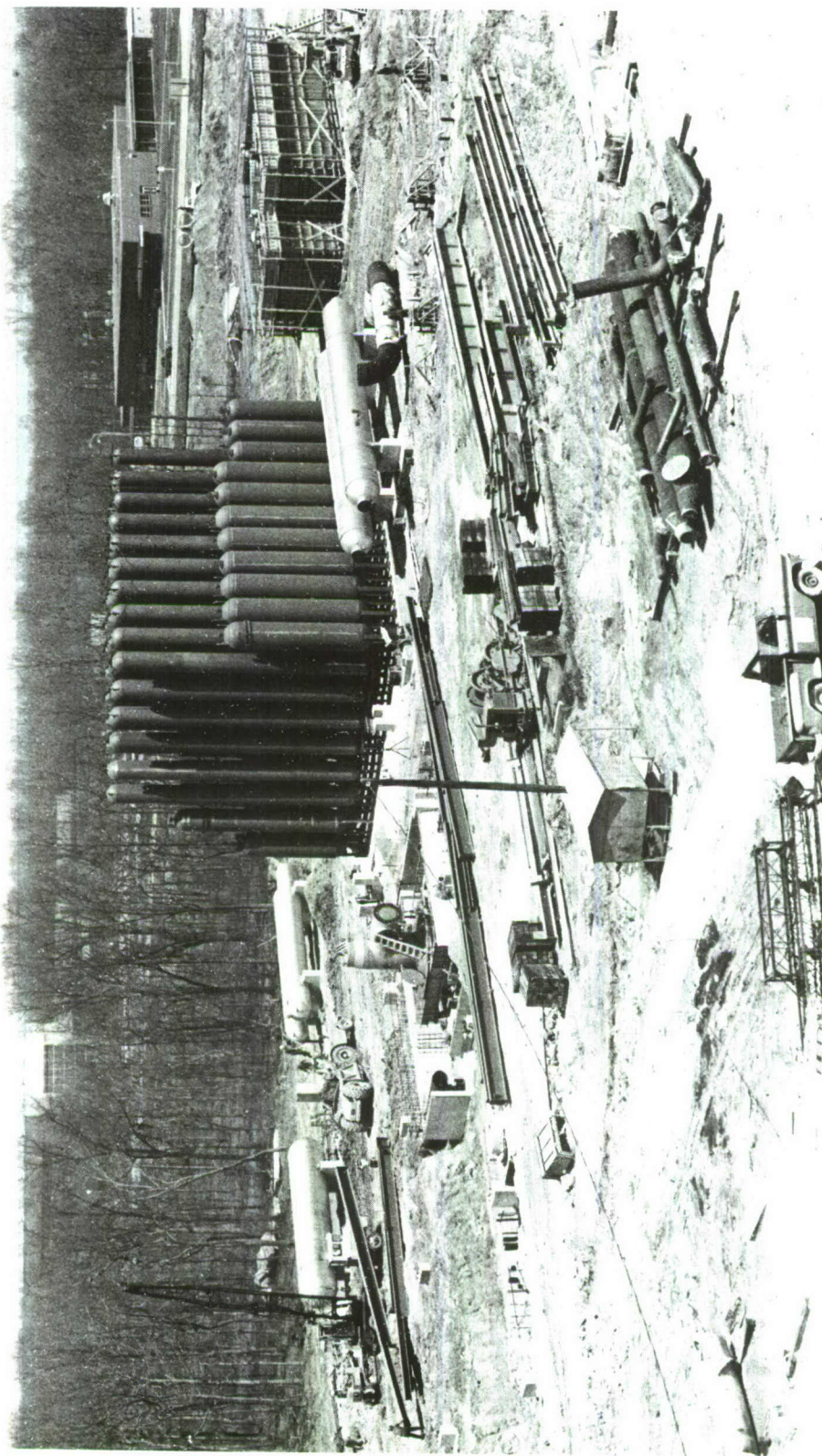
Figure 1. APTU Storage Tank Field
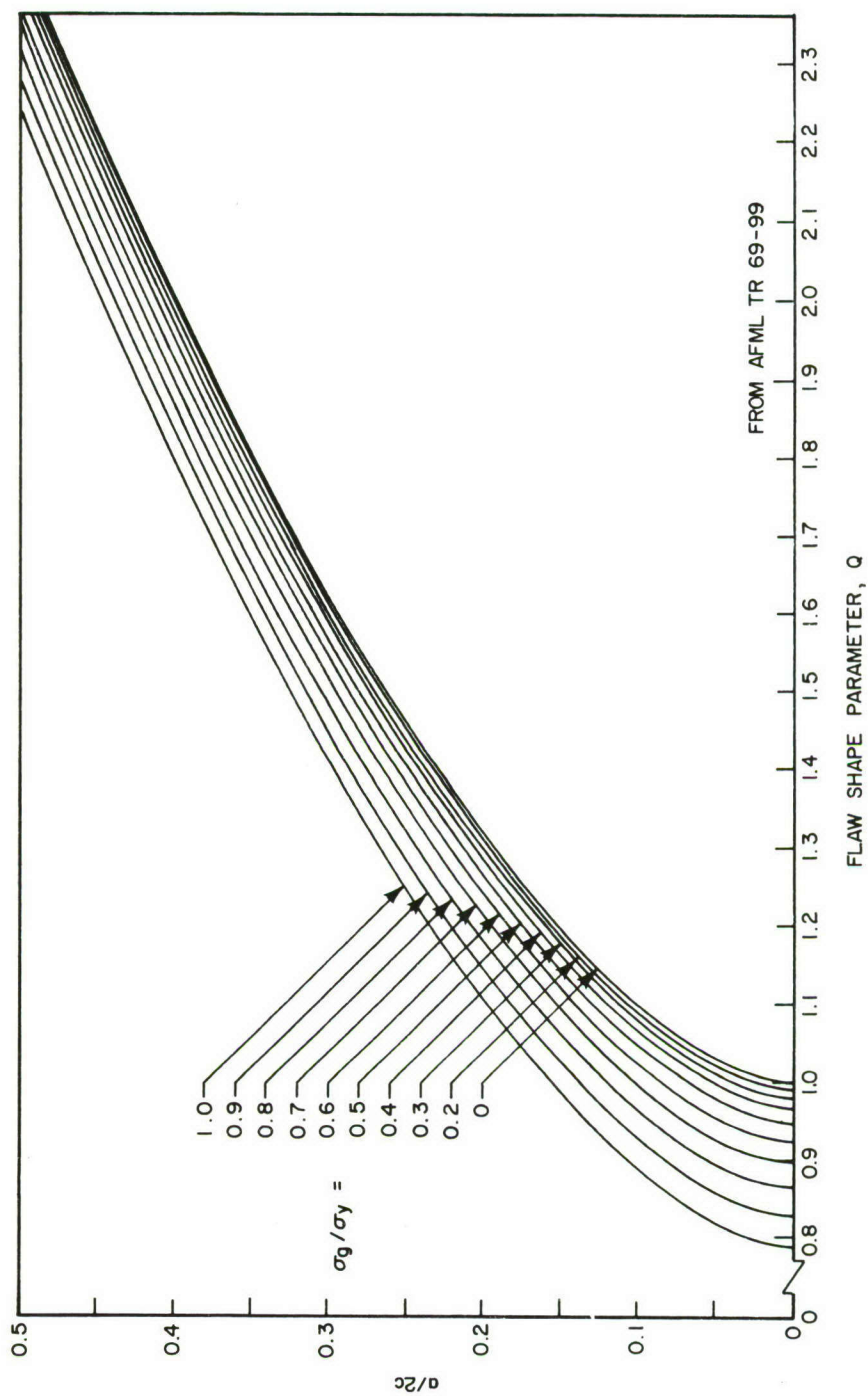
Figure 2. Shape Parameter Curves for Surface and Internal Flaws
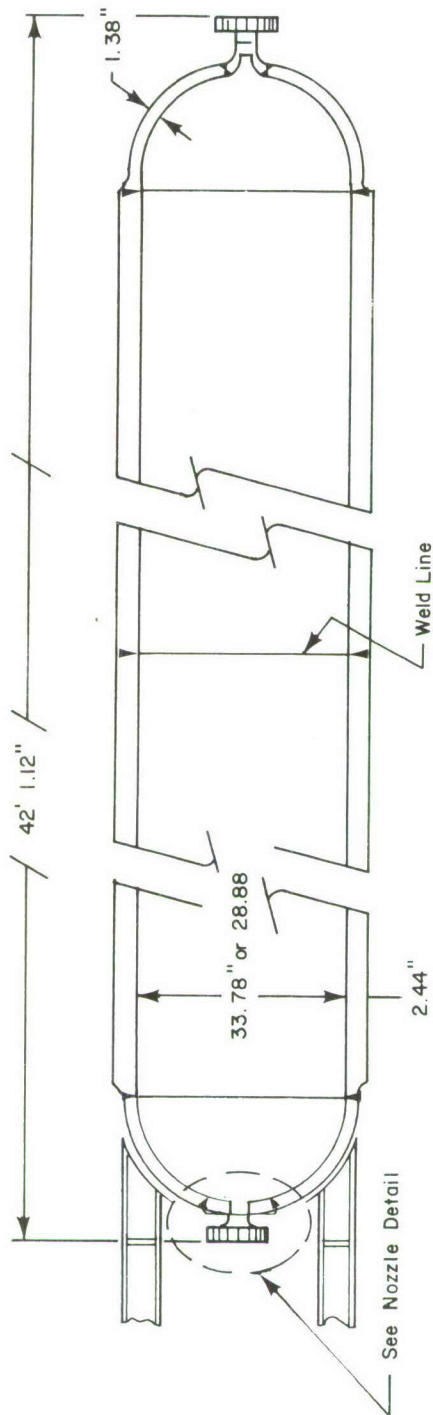
Materials:

Nozzles: SA350 LF3
(H.T. & Tempered
A-106)

Other: U.S. Steel T-1

Welds: Lincoln Elec.
L-60 or L-61

1.38"

42' 1.12"

33.78" or 28.88

2.44"

Weld Line

See Nozzle Detail

SA350-LF-3

T-1 Steel
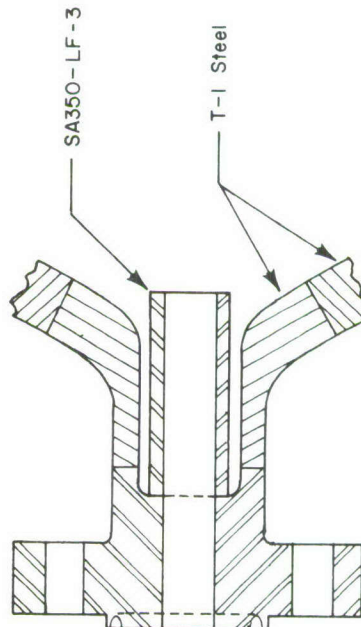
Nozzle Detail

Figure 3. Typical Foster-Wheeler High-Pressure Vessel Obtained
from Atlas Sites

21
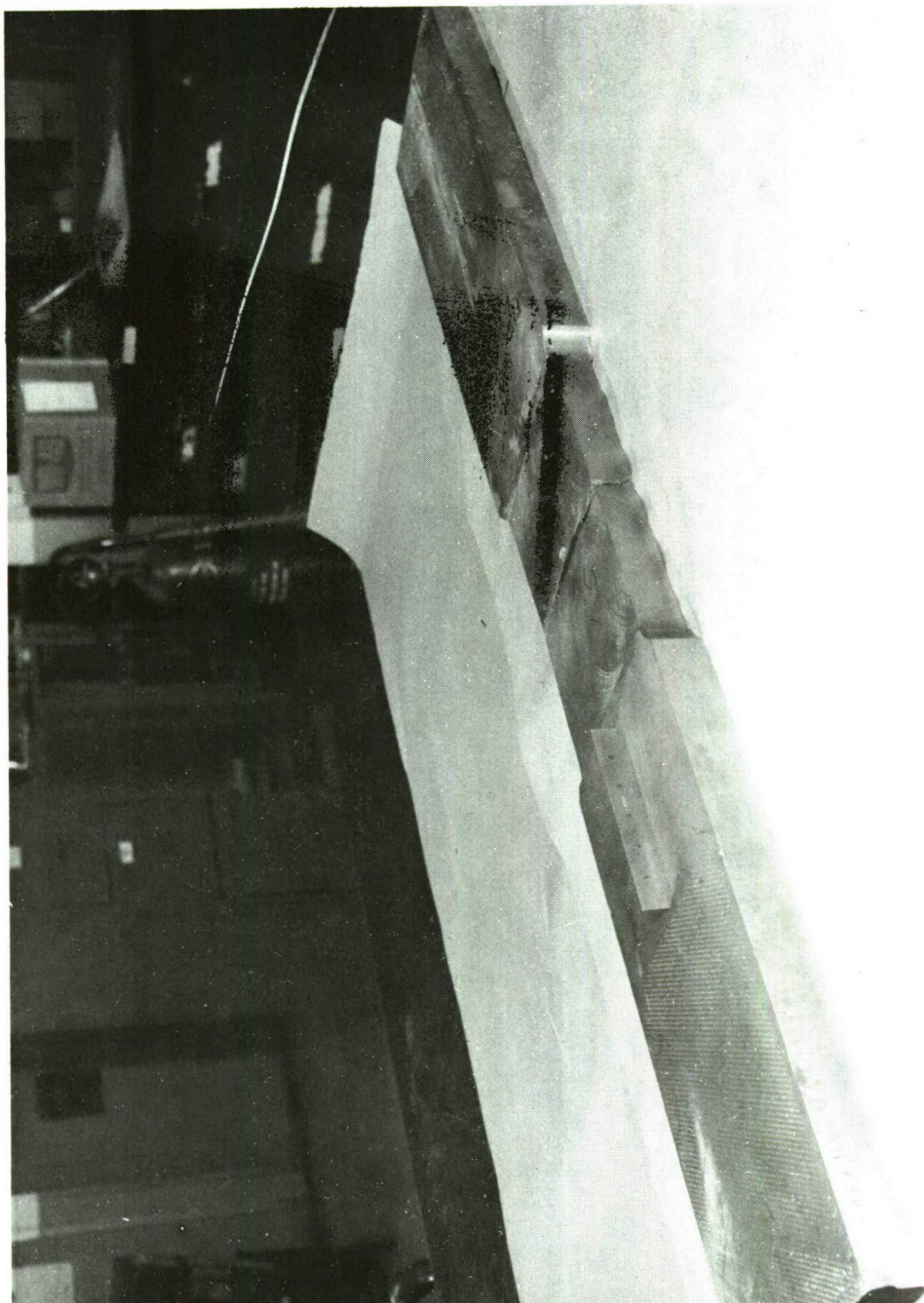
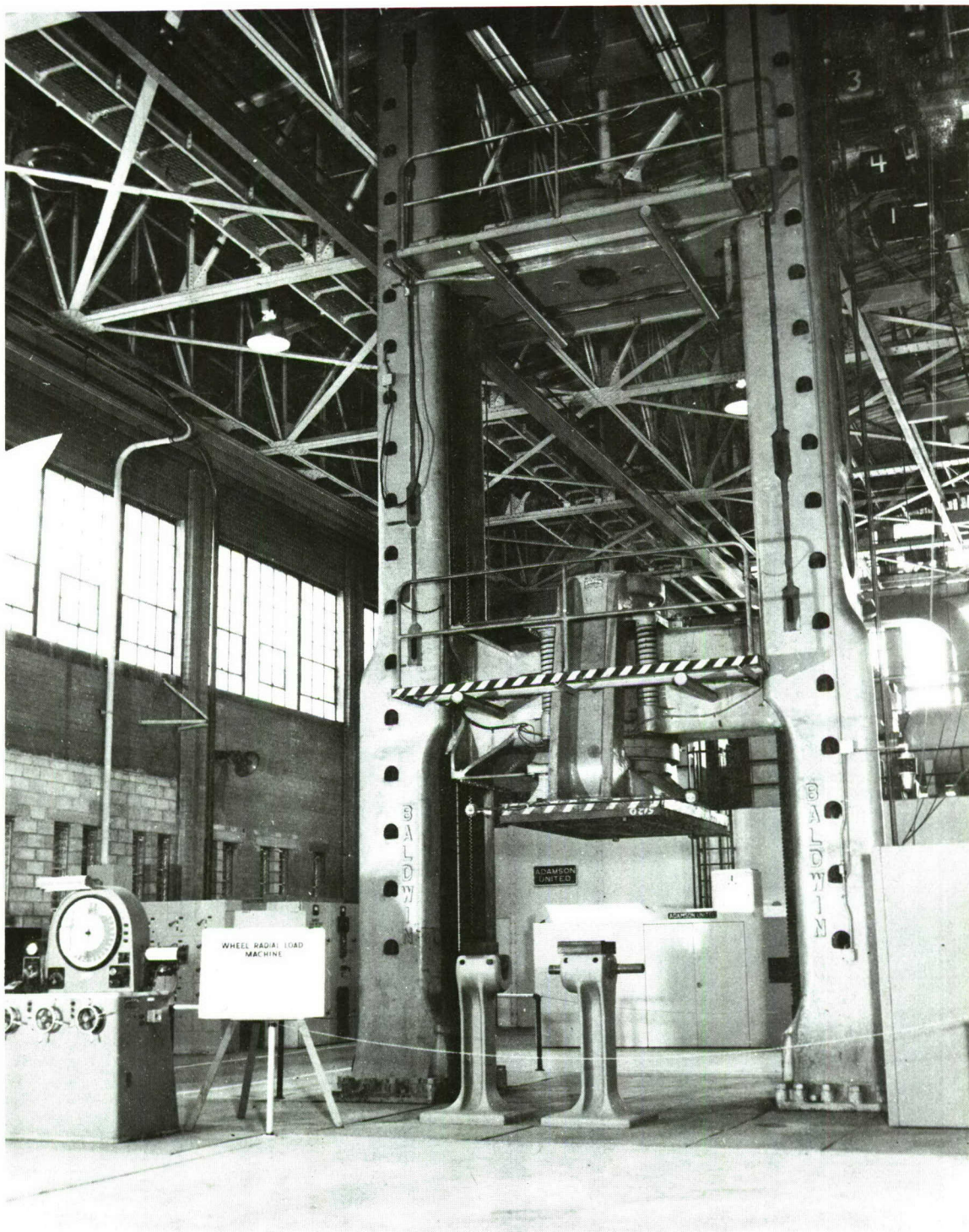Figure 4. Surface Flaw Specimen
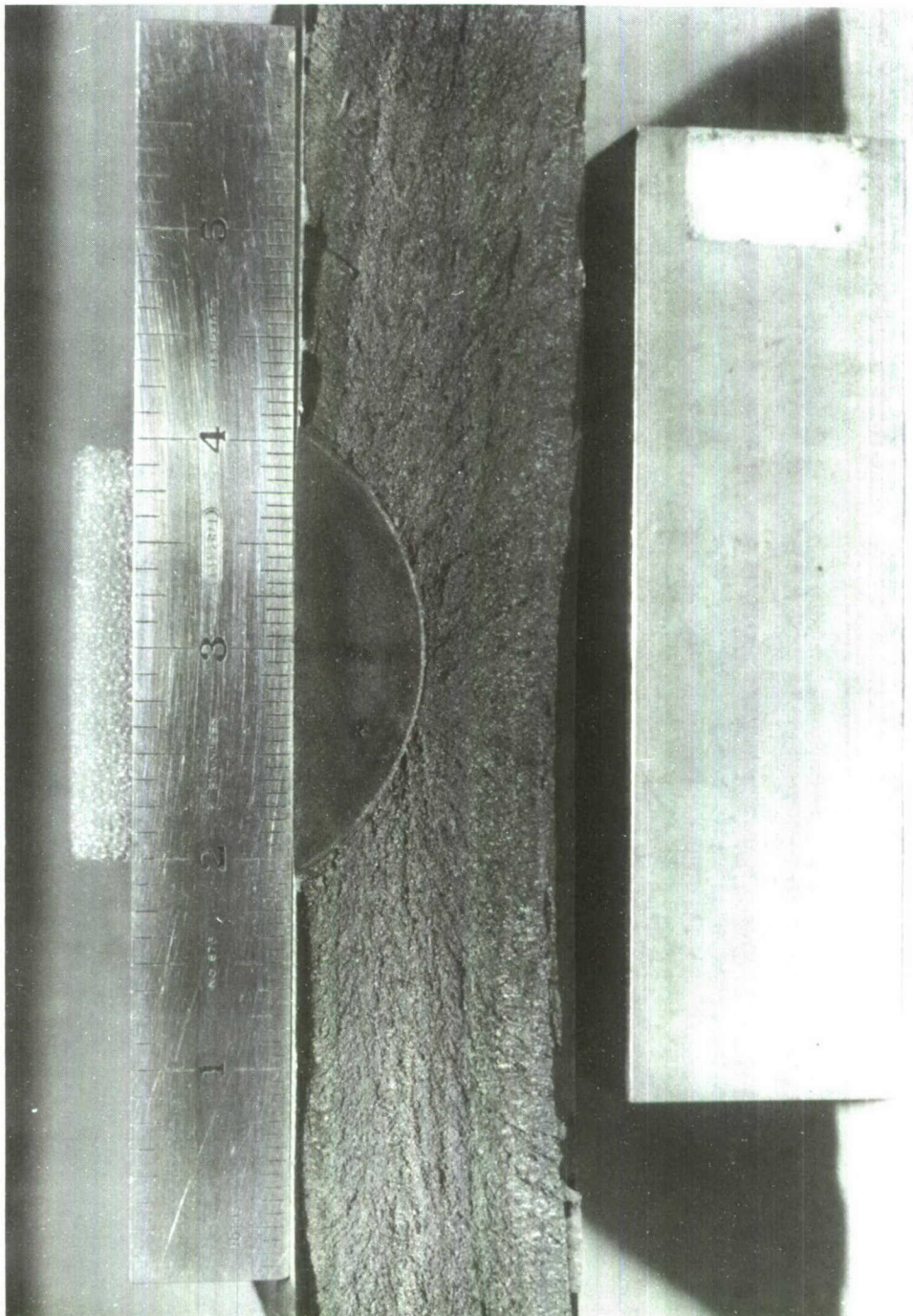
Figure 5. Flaw Shape EDM'd into Surface Flaw Specimen

Figure 6. AFFDL Test Machine
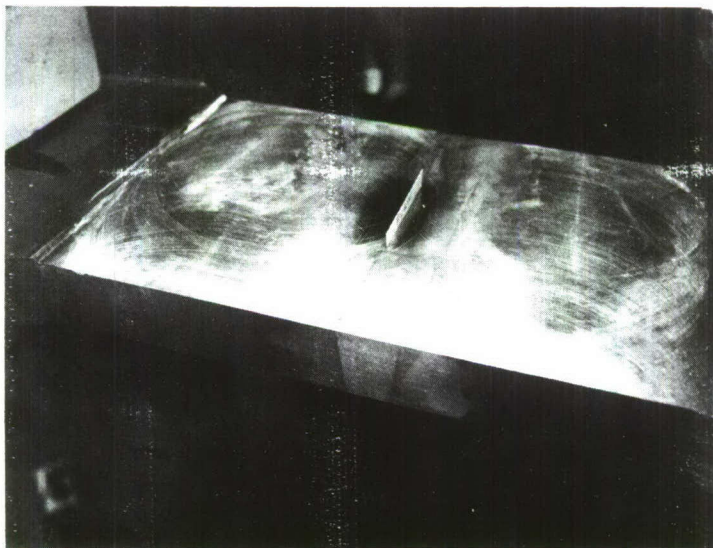
Figure 7. Etched Specimen Showing Weld Zone
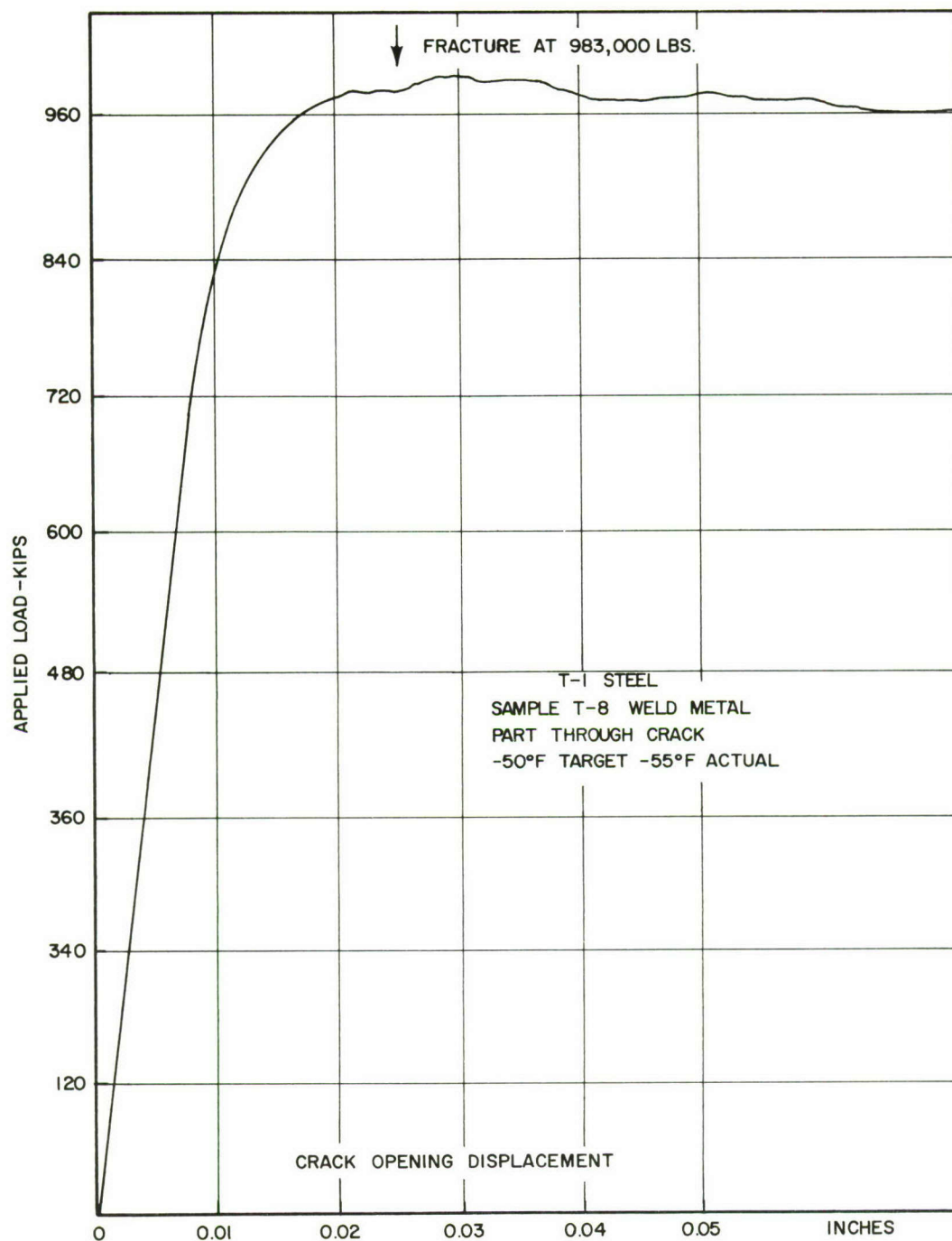
Figure 8. Typical Load versus Crack Opening Displacement Record
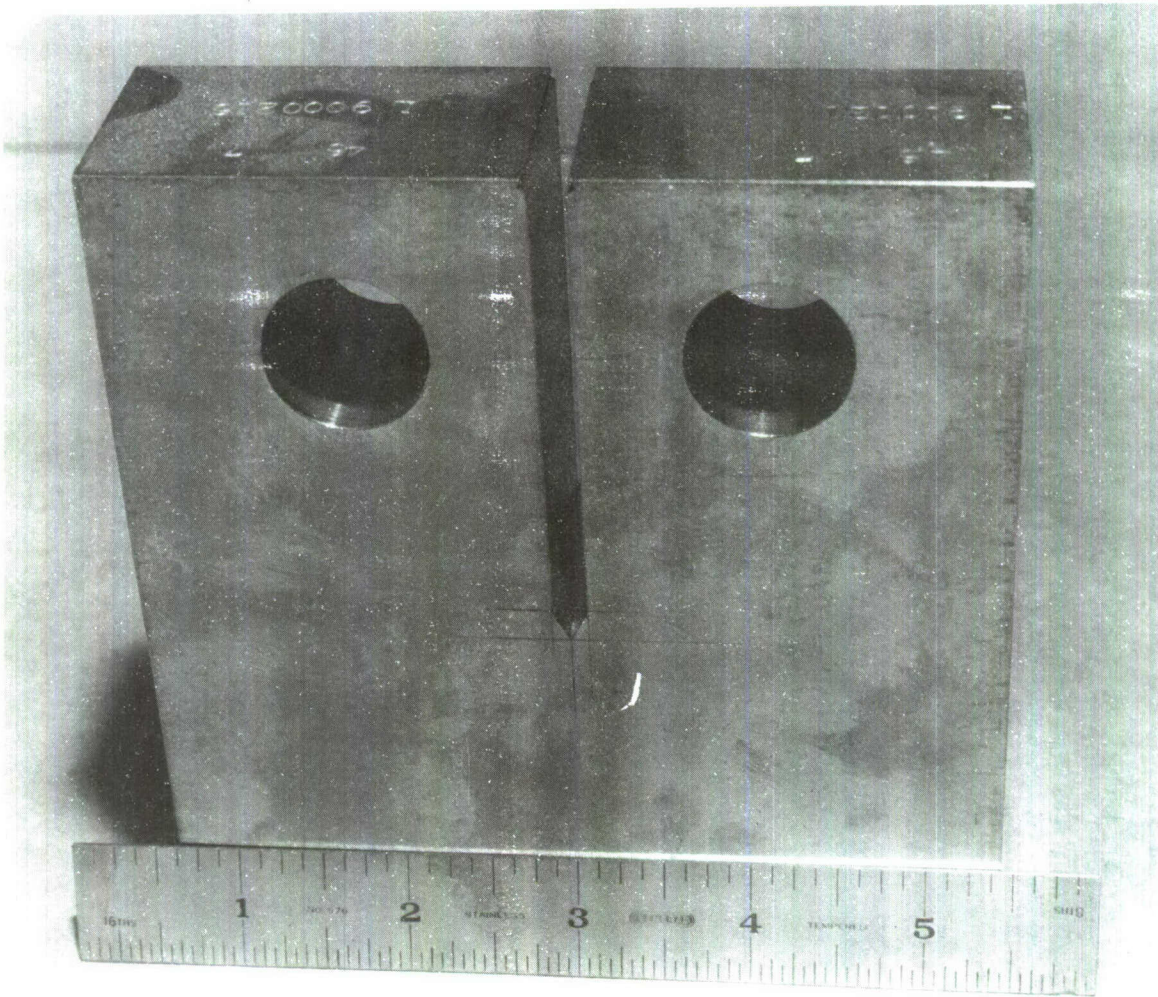
Figure 9. Compact Specimen Design
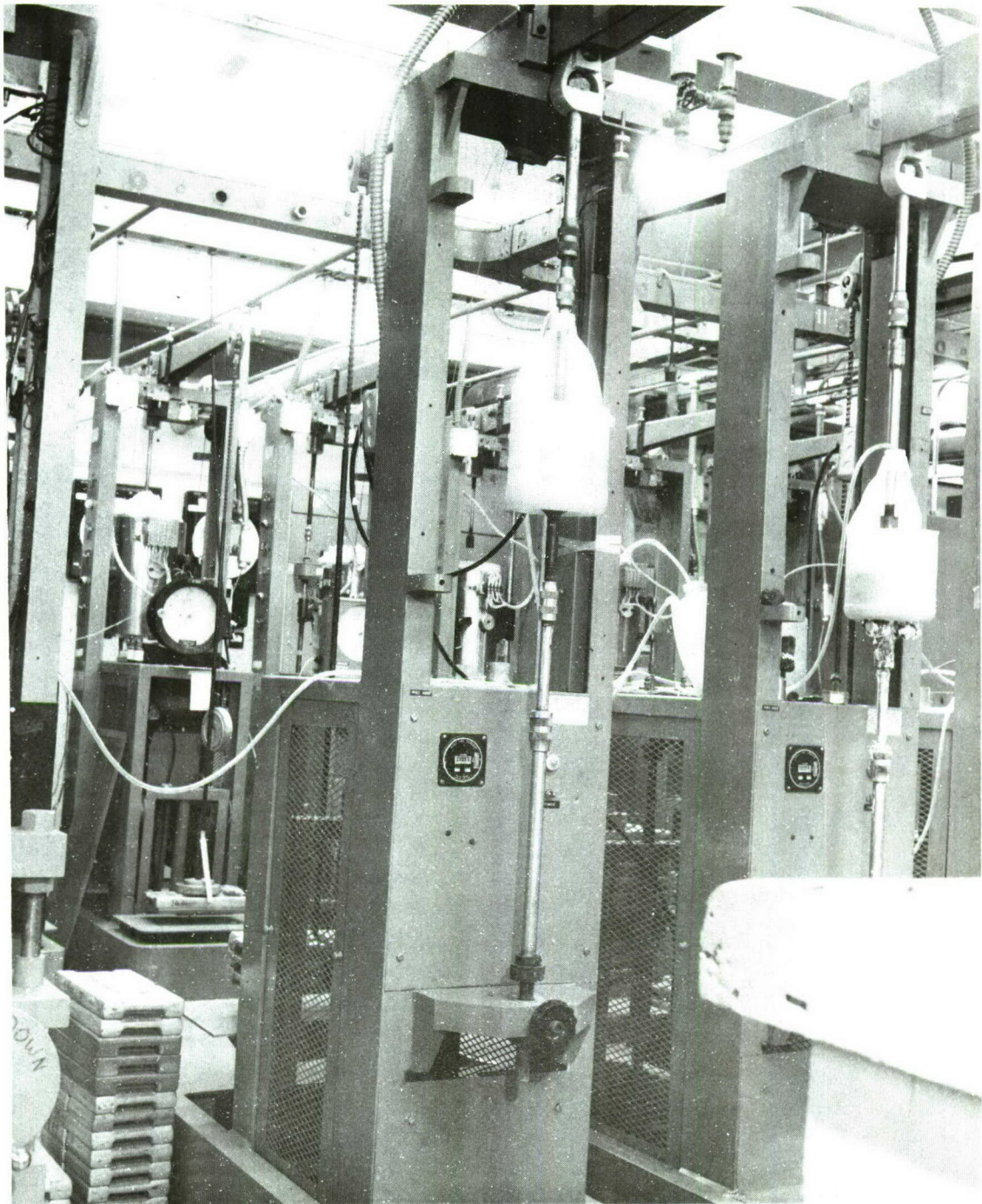
Figure 10. Stress Corrosion Test Set-Up
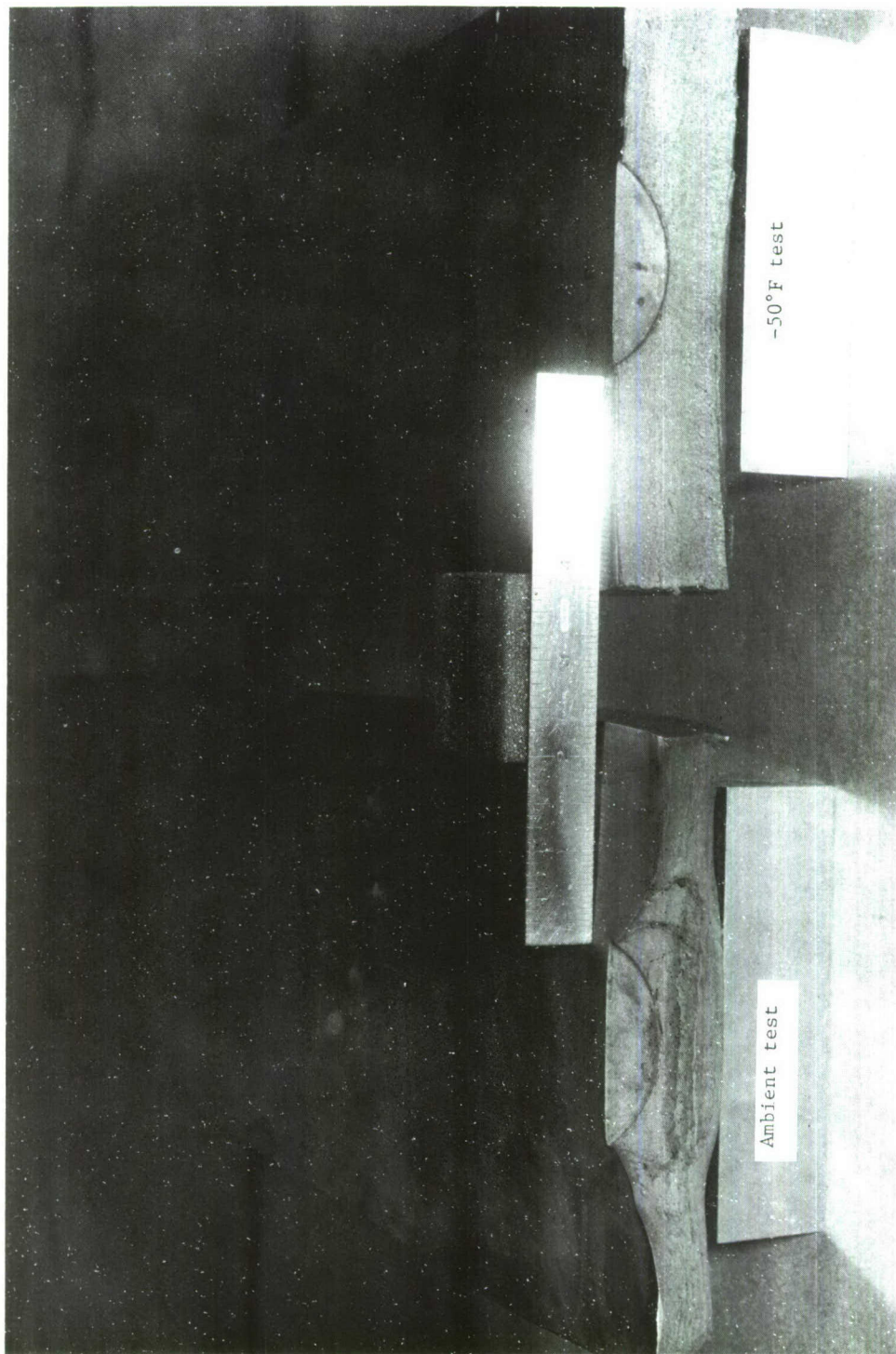
Figure 11. Fracture Surfaces from Ambient and -50°F Test Temperature
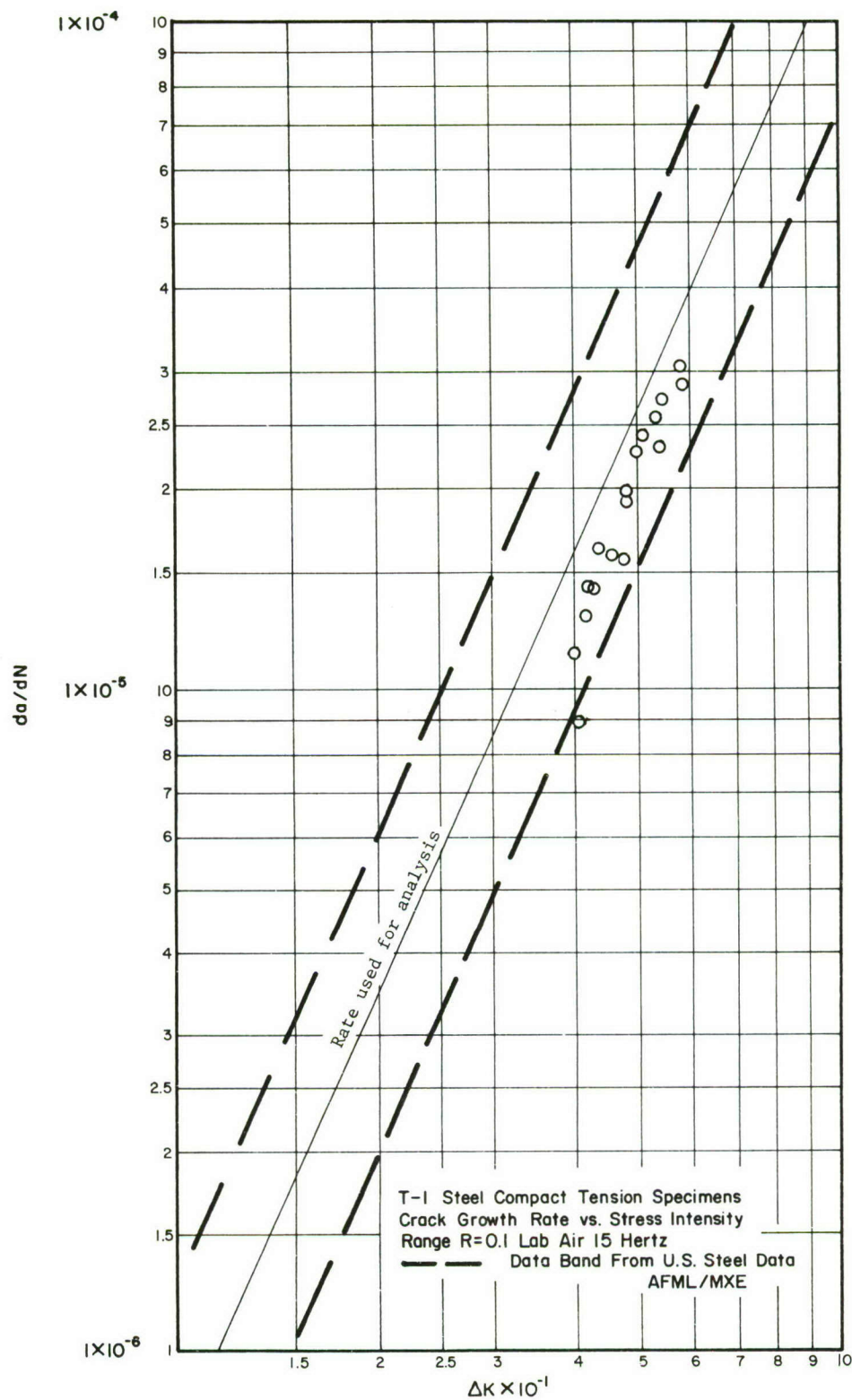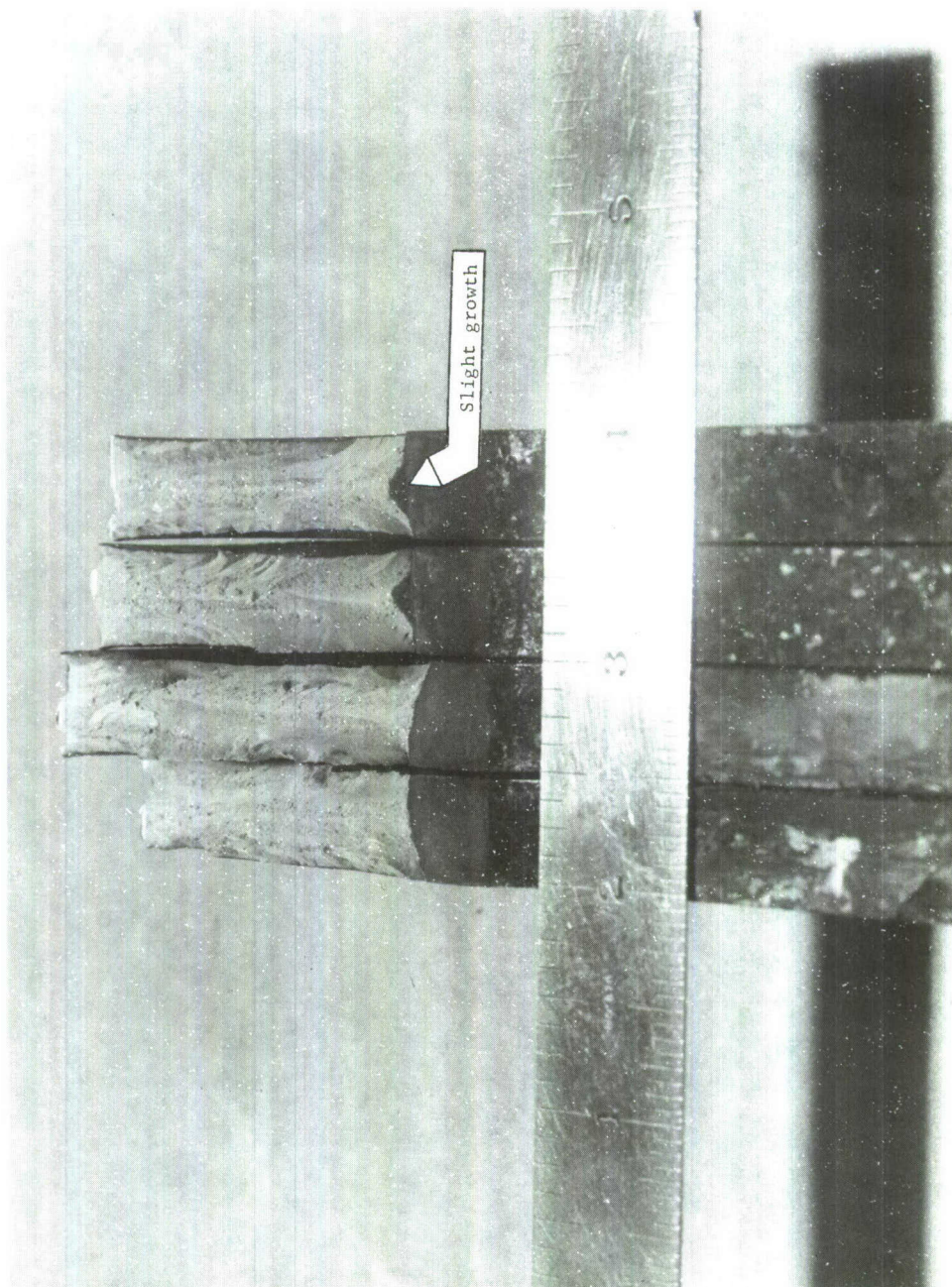
Figure 12. T-1 Steel Crack Growth Rate Data
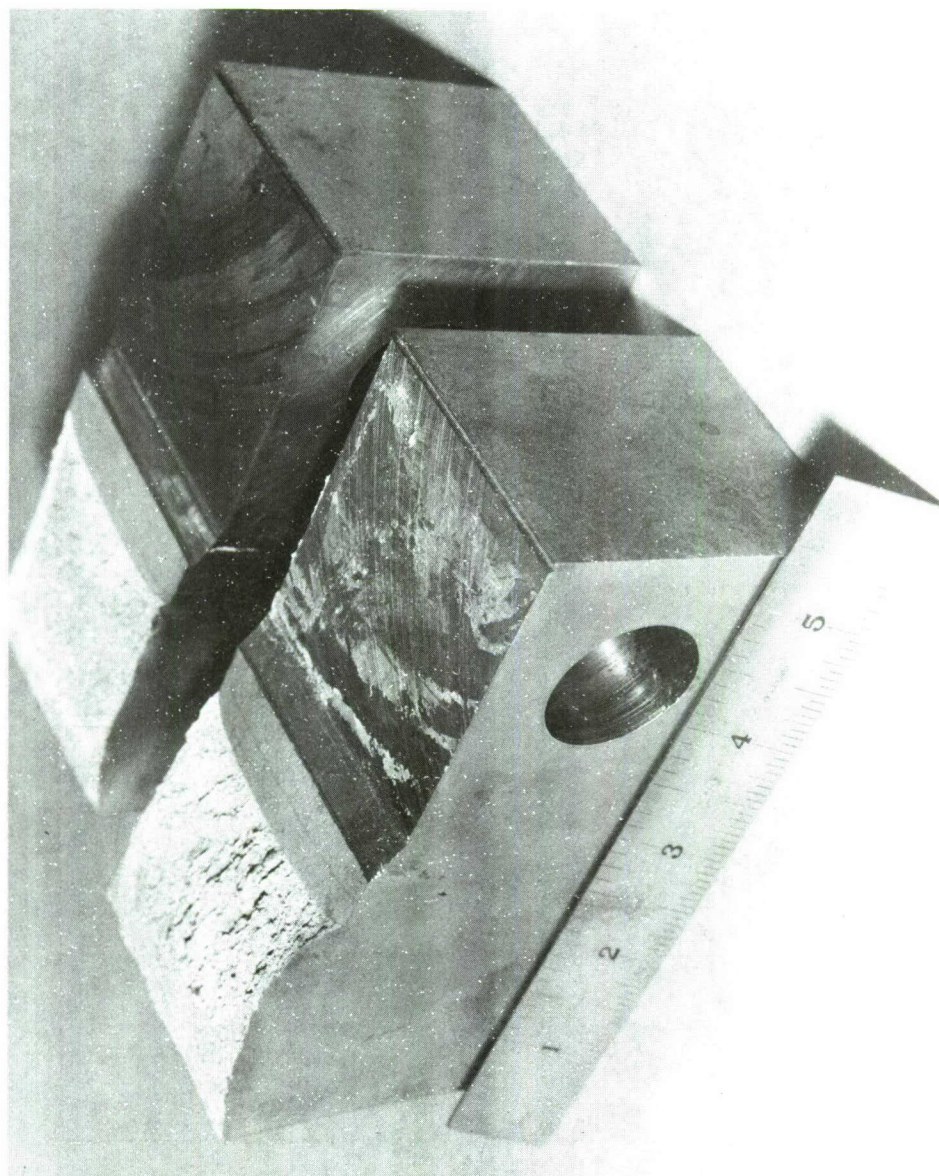
Figure 13. Stress Corrosion Fracture Surfaces T-1 Steel

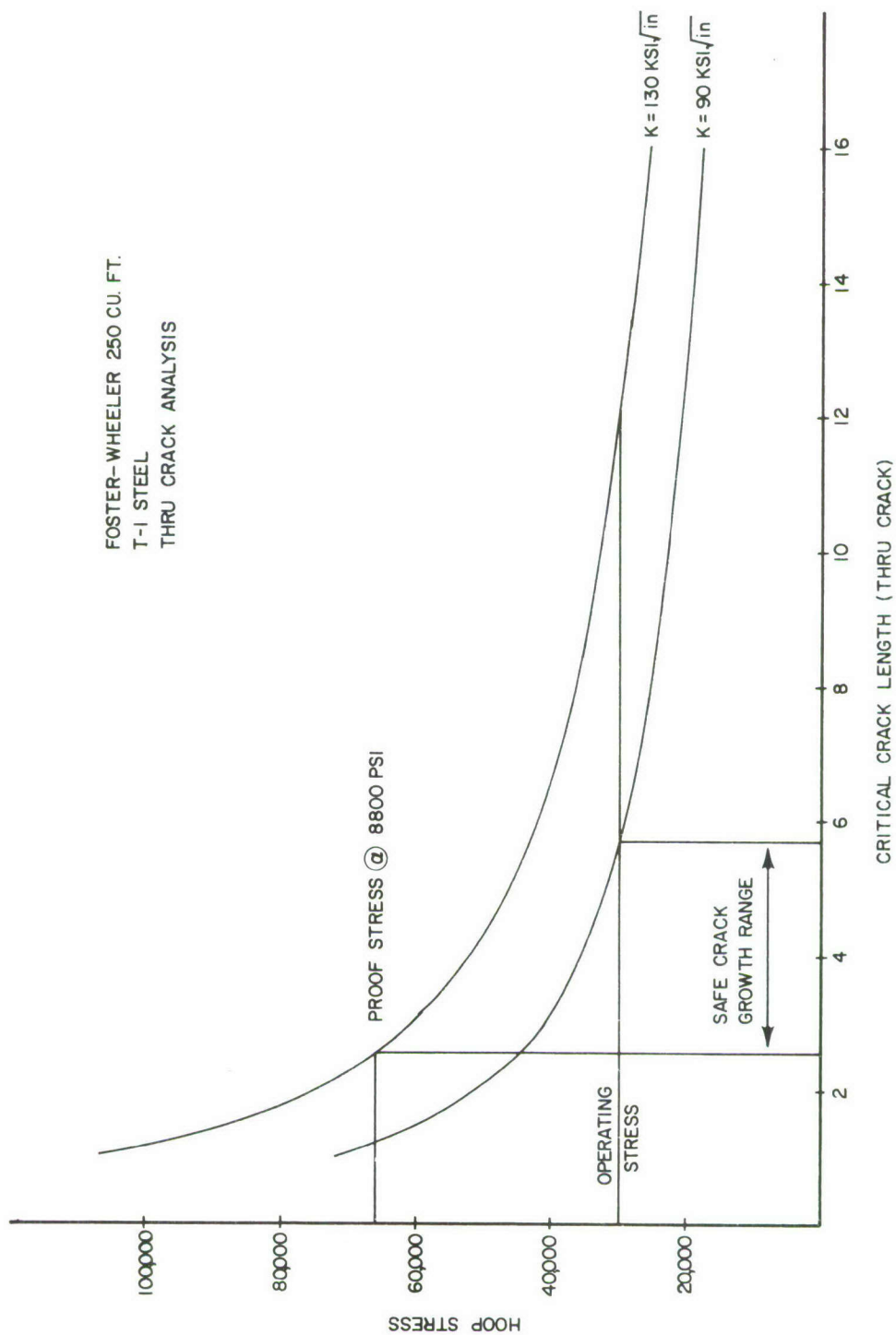Figure 14. Compact Specimens of A.O. Smith Head Material

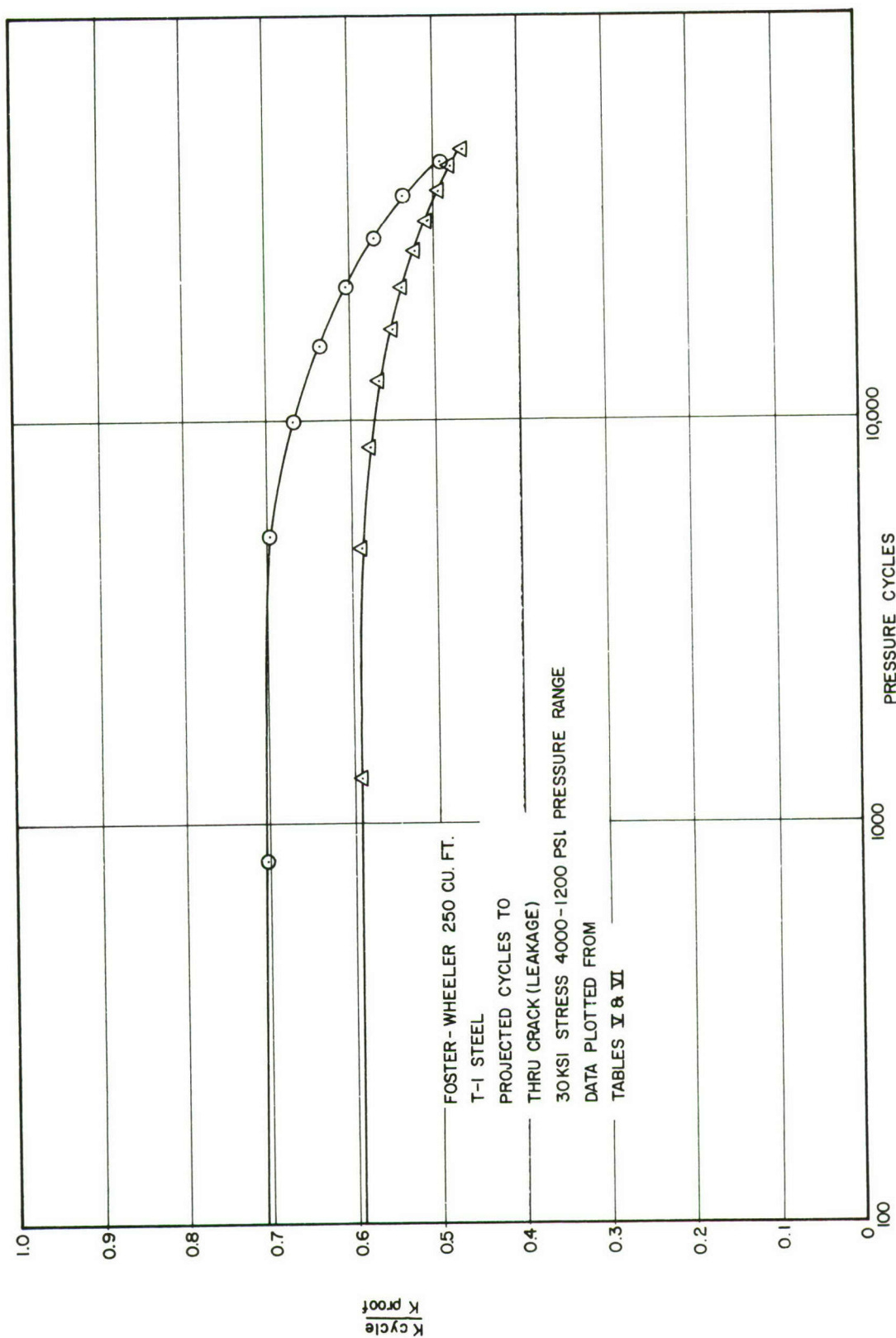Figure 15. Stress Level versus Critical Crack Length-Through Thickness Crack

Figure 16. K Proof/K Cyclic Ratio versus Pressure Cycles-Flaw Shape Variation
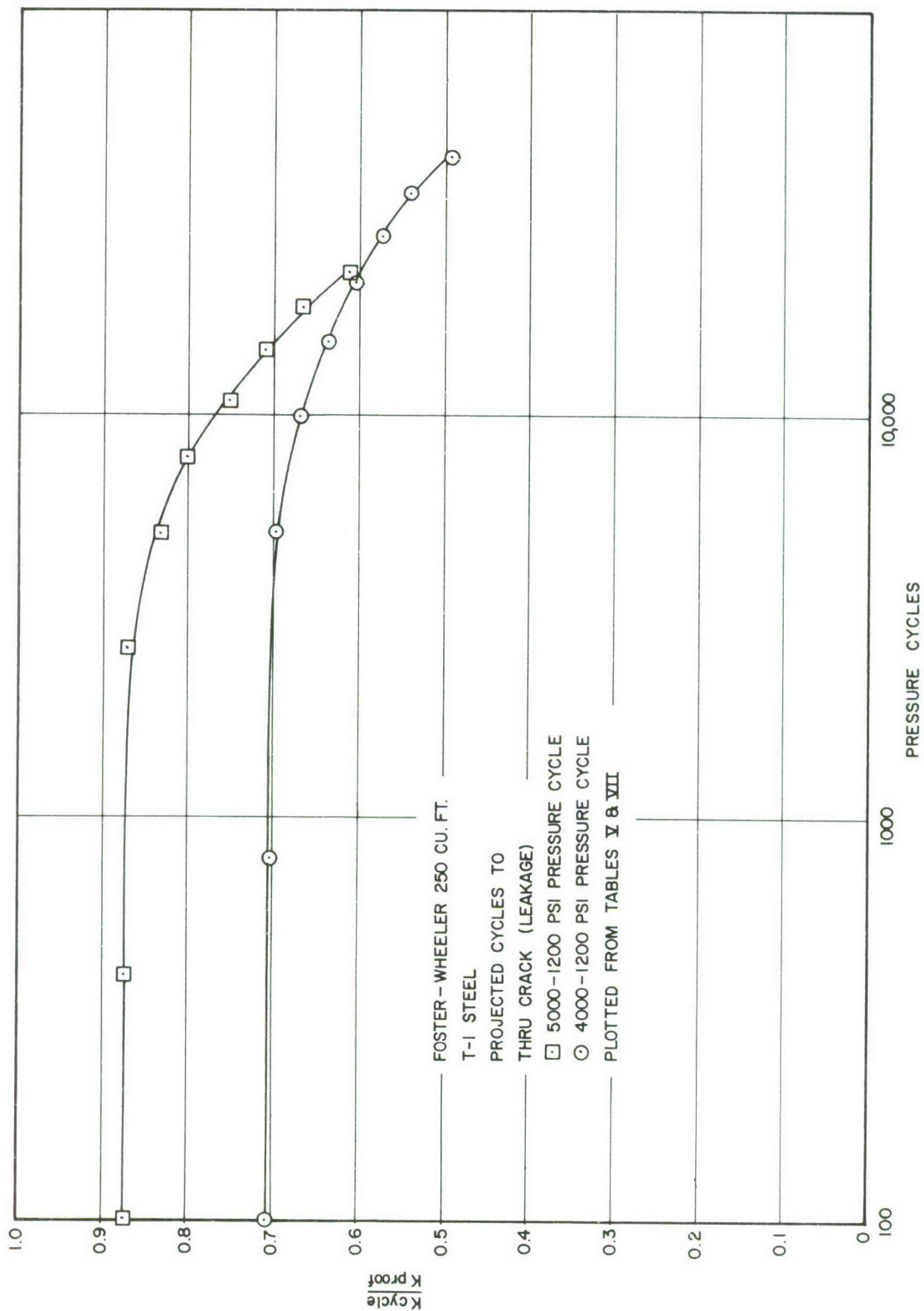⊙ a/2c = 0.1   △ a/2c = 0.25

Figure 17. K Proof/K Cyclic Ratio versus Pressure Cycles-Pressure Cycle Variation